Title: 3D particle-resolved aerosol model to quantify and reduce uncertainties in aerosol-atmosphere interactions

Principal Investigator: Matthew West
Mechanical Science and Engineering
University of Illinois at Urbana-Champaign
Address: 1206 West Green Street, Urbana, IL 61801
Phone: 217-333-2836
Email: mwest@illinois.edu

co-Principal Investigator: Nicole Riemer
Department of Atmospheric Sciences
University of Illinois at Urbana-Champaign

Field of Science: Atmospheric Sciences

1 Executive summary

This research aims to quantify key uncertainties associated with simulating aerosol-climate impacts. Aerosol particles influence the large-scale dynamics of the atmosphere and the Earth's climate because they interact with solar radiation, both directly by scattering and absorbing light, and indirectly by acting as cloud condensation nuclei. Their sizes range from nanometers to micrometers, and a major source of difficulty in understanding the aerosol climate impact is due to scale interactions because modeling those interactions is computationally expensive. The particle-resolved 3D model WRF-PartMC-MOSAIC, developed by the PI and collaborators, has the unique ability to track size and composition information on a per-particle level to address this problem, while remaining computationally feasible. In combination with efficient algorithms, a resource with the capabilities of Blue Waters is essential to perform WRF-PartMC-MOSAIC model simulations. This allocation has taken the significant step of taking WRF-PartMC-MOSAIC to the regional scale where the importance of aerosol composition in determining aerosol-cloud and aerosol-radiation interactions can be explored.

2 Research activities and results

Particle-resolved modeling provides insights into uncertainties regarding aerosol impacts on climate prediction. Many of the greatest challenges in atmospheric modeling and simulation involve the treatment of aerosol particles, ranging from the prediction of local effects on human health (Dockery and Pope, 1996) to the understanding of the global radiation budget via the aerosol indirect and direct effects (Stocker et al., 2013). Aerosol modeling has proved difficult because of the complex microscale physics of individual particles, which are not individually resolved in models — largely due to computational

constraints. Current methods of representing the high-dimensional and multi-scale nature of aerosol populations still make large simplifications. While this makes computation much cheaper, it introduces unknown errors into model calculations. This has far reaching consequences for the estimation of climate-relevant aerosol quantities, such as to calculate the particles' light scattering and absorption properties, as well as their abilities to form cloud droplets.

To overcome the current limitations in aerosol modeling, the particle-resolved aerosol model PartMC-MOSAIC (Riemer et al., 2009) was developed. This model stores the composition of many individual particles directly within a well-mixed computational volume. PartMC-MOSAIC was coupled with the Weather and Research Forecast (WRF) model, a state-of-the-art, publicly available fluid dynamics code for numerical weather prediction. The resulting WRF-PartMC-MOSAIC model uses a 3D Eulerian grid for the atmospheric fluid flow, while explicitly resolving the evolution of individual aerosol particles per grid cell. This next-generation model captures complex aerosol composition that current-generation models are unable to simulate.

Focus of this allocation. The work of this allocation focused on demonstrating the computational feasibility of the model to be run on Blue Waters for a realistic, regional-scale domain. We also tackled the science question of quantifying how important the details of aerosol composition are for estimating aerosol-climate interactions.

Blue Waters is essential as particle-resolved 3D atmospheric modeling is both compute-intensive and memory-intensive. A petascale resource with the capabilities of Blue Waters allows for using a cutting edge model that pushes science and computing by combining the large-scale features of state-of-the-art 3D chemical transport models with the process-level physical representation of box models. Simulations of aerosols at both a high spatial and compositional resolution requires tens of thousands of cores, fast interconnections between those cores, and sufficient memory per process. Given our problem size and the decomposed subdomain being as small as 1×1 in the horizontal, allocations on Blue Waters are necessary to achieve our scientific goals both now and in the future.

3 Code performance

WRF-PartMC performs well at the HPC scale. As a result of our previous Blue Waters allocations, the WRF-PartMC model was ported and evaluated at previously unobtainable scale. Previously, we tested both weak and strong scaling for future general allocations on the Blue Waters system. The results of this scaling are shown in Figure 1.

Stochastic algorithms make this model computationally feasible. Specifically, stochastic sampling techniques are used to simulated particle coagulation events, avoiding the testing for all possible events, and stochastic transport removes the necessity to track and update actual particle position. In addition, the model utilizes domain decomposition that can efficiently allow for parallelization. Given our problem size and the decomposed subdomain being as small as 1×1 in the horizontal, an allocation on Blue Waters is necessary to achieve our scientific goals. Despite increased complexity of the simulation on a realistic domain,

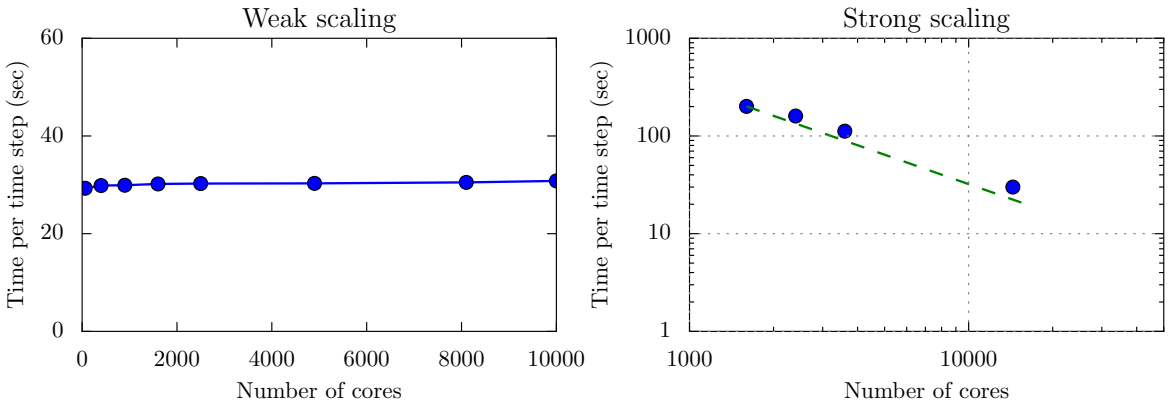

Figure 1: Scaling properties of the 3D particle-resolved WRF-PartMC on Blue Waters on XE nodes. Left: Data shows the weak scaling properties in terms of wall clock time per model time step. Each core was used to simulate a $1 \times 1 \times 60$ subdomain with 10 000 computational particles per grid cell. Right: Strong scaling performance using 10 000 computational particles per grid cell and an initial domain size of $120 \times 120 \times 60$. The problem size per core ranged from $3 \times 3 \times 60$ to $1 \times 1 \times 60$.

including complex wind patterns and spatially distributed emissions from many different sources of particles and trace gases, the simulation continues to scale well allowing for 1×1 columns per core.

4 Accomplishments and milestones

With this allocation, error quantification in climate-relevant quantities was possible for the first time for a realistic 3D domain. In addition to quantifying errors, model results will be useful in the future for benchmarking more simplistic aerosol models. Particle-resolved modeling allows for the full representation of aerosol composition. We developed a framework that takes mass-based aerosol emission fluxes, which are typically used for traditional chemical transport simulations, and converts them to number-based emissions fluxes, consistent with the PartMC framework. With this approach the source information of particles can be easily tracked. Figure 2 shows a subset of the tracked emission classes and their spatial distribution over the domain of interest.

We applied the model to the spatial domain of North Carolina. An ensemble of simulations was conducted over the domain in Figure 3. The model domain was $67 \times 53 \times 30$ with 12 km horizontal grid spacing. Figure 3 shows the total particle number emission rates, as well as the number of emission classes originating within each grid cell. Rural areas have few types of emission sources, while urban areas, such as Charlotte, contained as many as 25 different emission sources. Figure 4 shows the WRF simulated wind field that determines the stochastic advection of aerosol particles (left) after 6 hour of simulation, and the horizontal distribution of number concentration of particles containing black carbon near the surface (right).

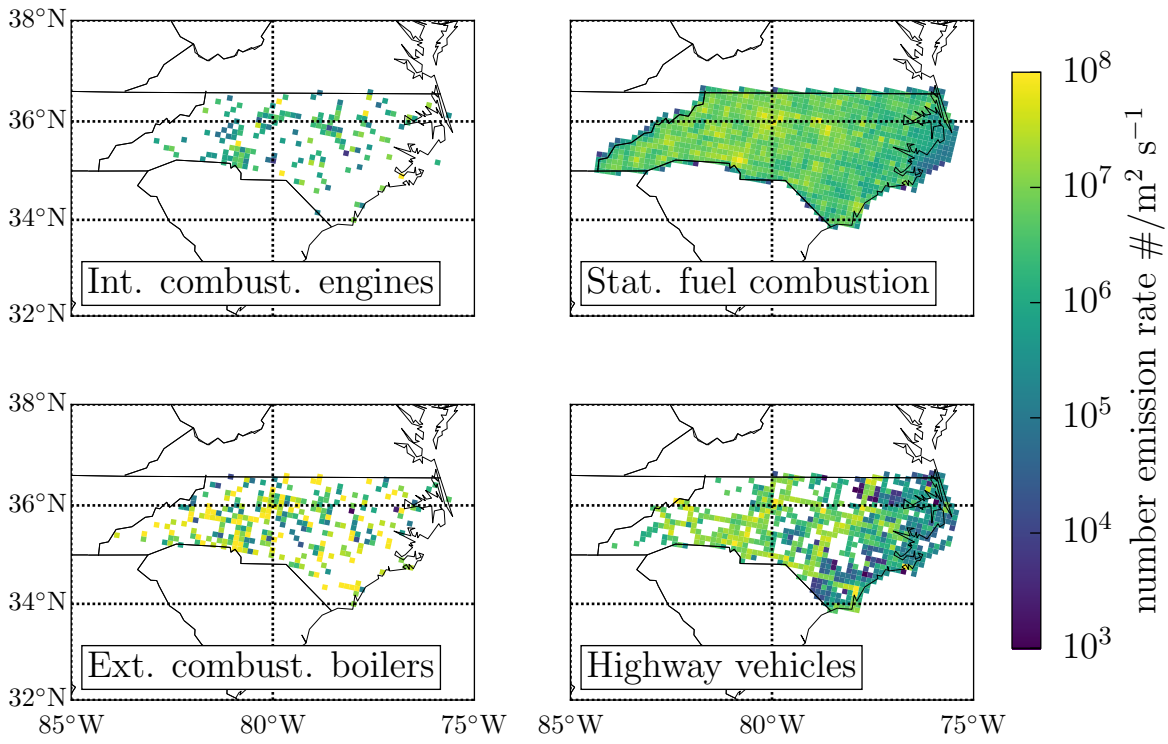

Figure 2: Emission number flux for four different sources: Internal combustion boilers, off-highway vehicles, external combustion boilers and highway vehicles. Each emission source has its unique composition profile.

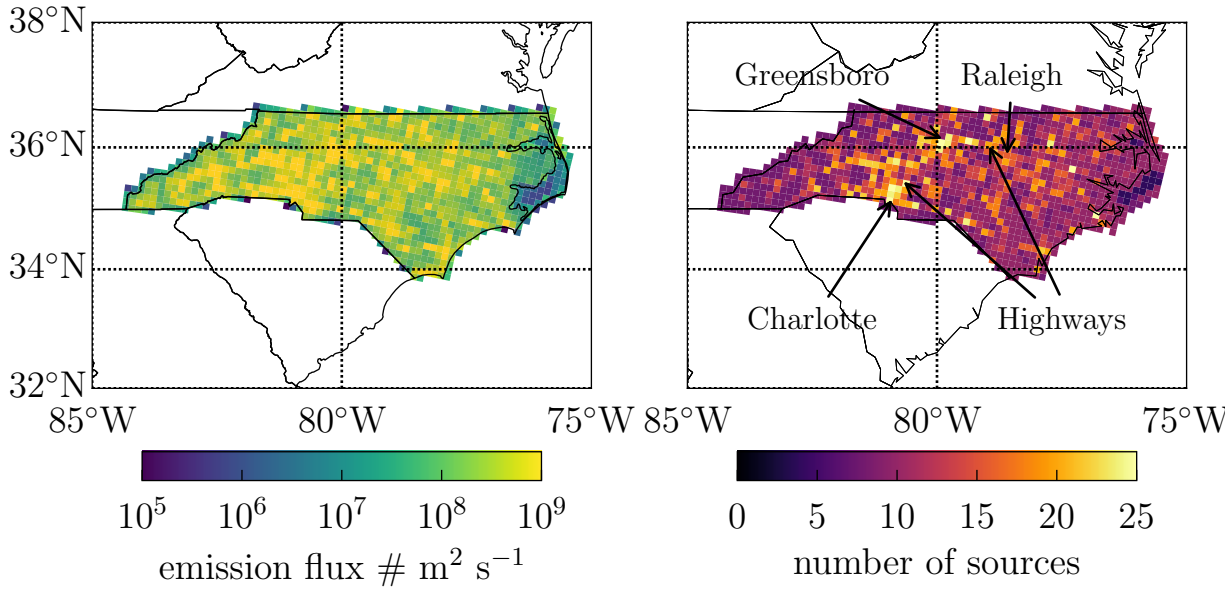

Figure 3: Total particle number emission flux (left) and total number of tracked source modes (right). The urban areas show a larger particle number emission flux as well as a larger number of particle sources per grid cell.

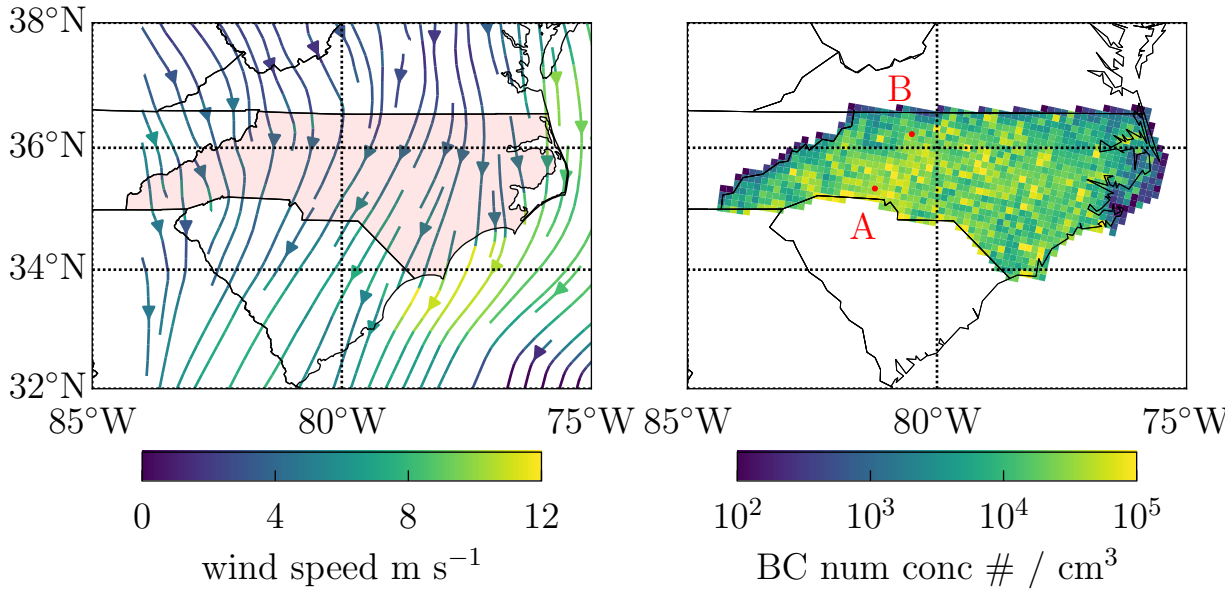

Figure 4: Wind field after 6 hour of simulation (left) and corresponding horizontal distribution of simulated number concentration of black-carbon-containing particles near the surface (right).

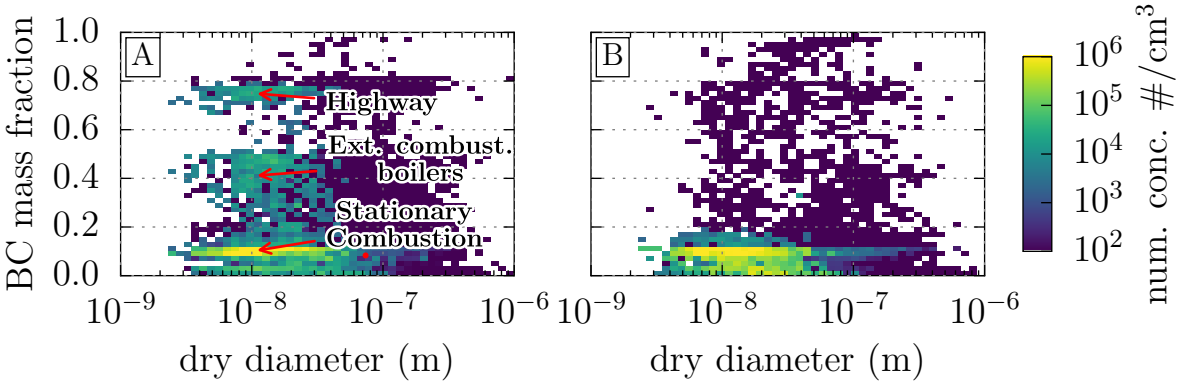

Figure 5: 2D histograms of black carbon mixing state at points A and B.

The WRF-PartMC-MOSAIC model captures the continuum of aerosol compositions. As an illustrative example, Figure 5 shows the aerosol composition at points A and B, marked in Figure 4. At Point A, which is located near an urban area, we find a wide variety of particle compositions. Emission classes that contain black carbon at this location are labeled in Figure 5 with highway vehicles containing the largest black carbon mass fractions. At Point B, which is located upwind of areas of higher emissions, less freshly emitted black carbon particles are present.

Tracking contributing sources to aerosol number concentration. Figure 6 shows the associated number concentration of particles that contain some fraction of mass from a particular source, contrasting Points A and B. At Point A, which is located downwind from major interstates in North Carolina, we find a large contribution from highway vehicles. This source is absent at Point B, which is not located in the vicinity of a highway.

As the model tracks composition and source information of thousands of computational particles per grid cell, individual particles may also be explored such as shown in Figure 7. Here a particle with a particular size and black carbon mass fraction has been selected, marked with a red dot in Figure 5. In Figure 7 (left) the mass of each constituent species is shown for a single particle with the chosen particle containing primarily dust, emitted organic and black carbon and has undergone chemical transformation due to condensation of nitrate. Figure 7 (right) shows the original sources of this particle that formed from coagulation events to contain portions from industrial processes and waste burning. These capabilities will be useful in the future for quantifying how much individual source categories are contributing to the pollution at a certain location.

Quantifying the importance of mixing state for CCN activity. To evaluate CCN prediction errors, CCN concentrations were compared from a particle-resolved simulation to a composition-averaged simulation. The composition-averaged simulation mimics the aerosol representation in traditional aerosol models by assigning identical, averaged composition to particles having the same size. By comparing model results using the two representations, the effect of aerosol mixing state on model errors in CCN concentrations was determined. Figure 8 (left) shows the over- and underestimation of CCN number concentrations when

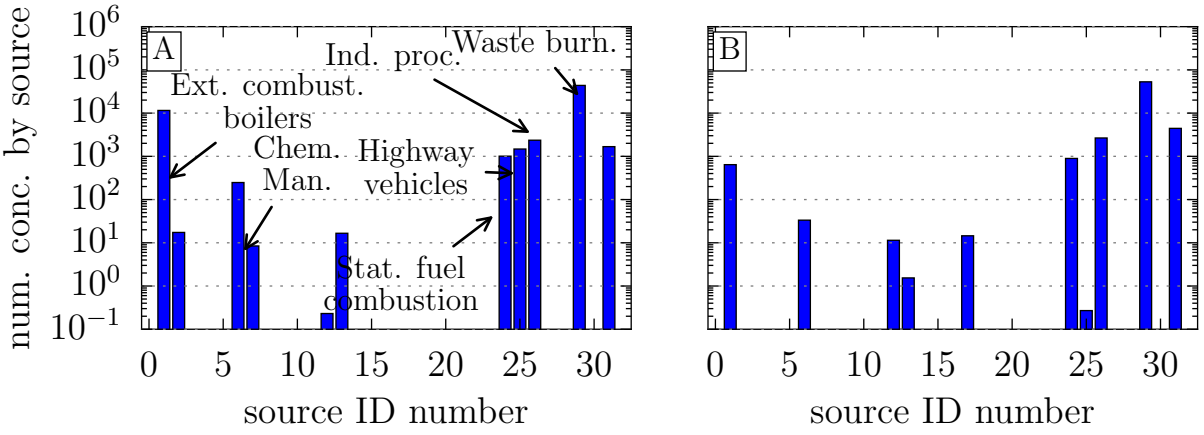

Figure 6: Particle source information of aerosol populations at points A and B. The originating source of all particles is tracked throughout a simulation.

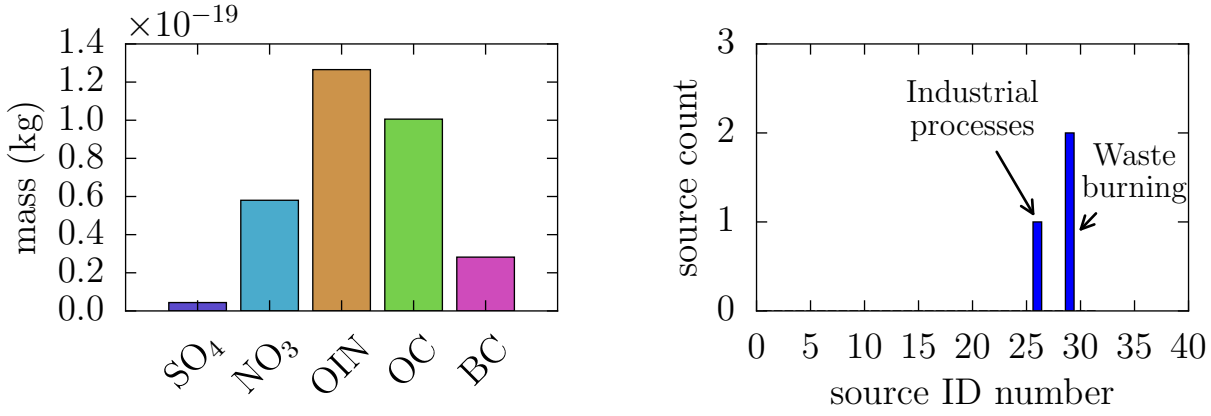

Figure 7: Composition information (left) and source information (right) of a single particle at point A.

mixing state information is ignored.

Figure 8 (right) shows the critical supersaturation of particles before and after composition averaging. The red and blue regions represent particles that activate in one case but not the other, leading to a mis-categorization of the particles. Composition-averaged particle populations may have higher CCN number concentrations as particles that are hydrophobic become hydrophilic when artificially coated with inorganics (such as nitrate and sulfate). This results in particles activating when aerosol mixing state is assumed to be internally mixed (particles in the blue region). Likewise, a redistribution of composition may result in particles no longer activating. The CCN error is determined by the difference in number concentration of particles in the blue and red area. The two effects may lead to a partial or total cancellation. As a result, we may obtain a small error, but for the wrong reasons.

How internally mixed is the aerosol over our modeling domain? The mixing state parameter χ, as described in Riemer and West (2013), quantifies the extent to which the particle population is internally mixed. Specifically, the mixing state parameter χ is given by the relationship, $\chi = (D_\alpha - 1)/(D_\gamma - 1)$, where D_α is the alpha diversity and D_γ is the gamma diversity. Alpha diversity, D_α, reflects the average per-particle effective number of species in the populations. Values of D_α can fall in the range $1 \leq D_\alpha \leq A$, where A is the number of species. $D_\alpha = 1$ when all particles are composed of a single species, while $D_\alpha = A$ when all particles have identical mass fractions. The gamma diversity D_γ reflects the bulk population species diversity. Values of bulk species diversity range from $1 \leq D_\gamma \leq A$, where $D_\gamma = A$ when all species in the bulk appear in equal amounts. The values of χ range from 0 for a fully externally mixed particle population to 1 for a fully internally mixed particle population. Current-generation aerosol models used in climate models commonly assume internal mixtures. This assumption may cause large errors in their estimation of climate impacts when the aerosol is in reality more externally mixed.

Figure 9 shows horizontal distributions of the mixing state parameter. This tells us how internally or externally mixed the aerosol is over the entire domain. We can define different variants of the mixing state index, as illustrated in Figure 9A, B, and C. Figure 9A shows the mixing state based on chemical composition. In the central regions emission rates are higher and from many divers sources as shown in Figure 3. This results in a lower mixing state parameter, signifying a more externally mixed aerosol population. Figure 9B depicts the mixing state parameter based on the mixing of hydrophobic and hygroscopic aerosol material, and Figure 9C is the mixing state parameter based on the mixing of absorbing and non-absorbing aerosol material. Both Figure 9B and Figure 9C show more externally mixed populations in the central region of the state, while in the east and west part of the state the aerosol is rather internally mixed.

5 Next Generation Work: Track-1 systems in 2019-2020.

The next-generation Track-1 systems will allow for improved resolution simulations and model improvements for physical processes. Higher detail may consist of a variety of possi-

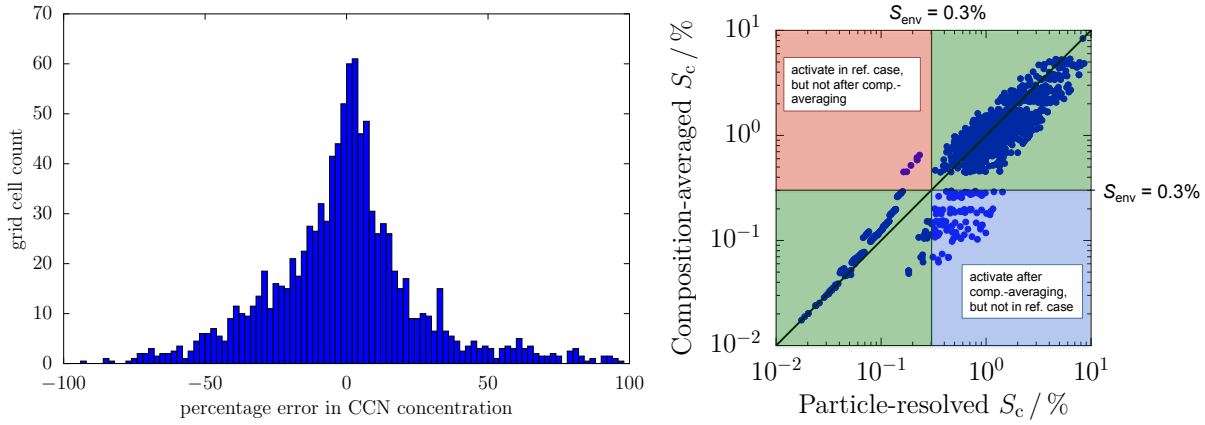

Figure 8: (left) Percentage error in CCN number concentrations when aerosol mixing state is neglected when compared to the particle-resolved representation. (right) Critical supersaturations of particles when particle-resolved and when mixing state is neglected. Red region indicates when underestimation occurs, and blue region indicates when overestimation occurs.

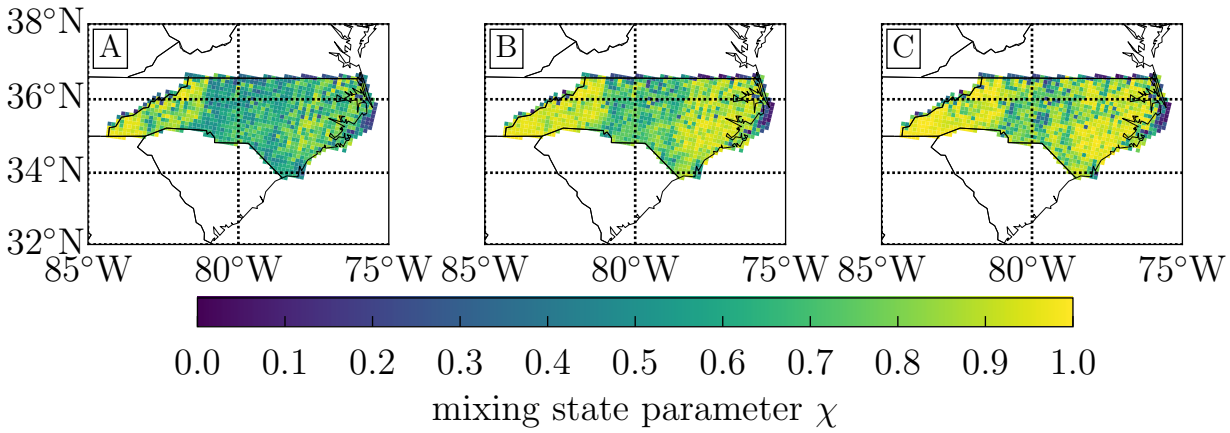

Figure 9: Map of mixing state parameter with (A) χ (mixing state index based on chemical composition), (B) χ_{CCN} (mixing state index based on the mixing of hydrophobic and hydrophilic materials. This is useful for investigating CCN properties), and (C) χ_{optical} (mixing state of based on the mixing of absorbing and non-absorbing material. This is useful for investigating optical properties.)

ble model refinements including (1) the domain may be represented with a higher-resolution spatial grid, (2) more emission source classes may be tracked, (3) increased number of simulated particles per grid cell, and (4) inclusion of more advanced aerosol chemistry modules.

This would facilitate comparisons between particle-resolved simulated results and field measurements of per-particle aerosol composition. Due to the microscale nature of aerosols, modeling efforts are particularly important in combination with field measurements and laboratory studies, to advance process-level understanding of the key interactions among aerosols, clouds and radiation, with the ultimate goal of reducing the uncertainty in global and regional climate simulations and projections.

6 Publications and products

- Telluride Workshop on Aerosol-Cloud Interactions, June 29, 2016, oral presentation by N. Riemer titled "Towards a multiscale aerosol modeling hierarchy".
- Invited seminar in the Computational Science and Engineering seminar series, October 26, 2016, by N. Riemer, titled "Stochastic Particle-Resolved Models for Atmospheric Simulation".
- American Meteorological Society 97th Annual Meeting 19th Conference on Atmospheric Chemistry, January 26, 2017 oral presentation by J. Curtis titled "A 3D Particle-resolved Model to Represent Aerosol Mixing State".
- Poster at the Department of Energy 2017 Atmospheric Radiation Measurement/Atmospheric System Research (ARM/ASR) PI Meeting March 13–16, 2017, presented by J. Curtis, titled "A 3D Particle-resolved Model to Quantify Spatial and Temporal Variations in Aerosol Mixing State".
- Model development paper in-preparation for submission to *Geophysical Model Development* regarding the extension to 3-D spatial domains. J. Curtis, N. Riemer, and M. West, Importance of resolving aerosol mixing state: insights into cloud condensation nuclei activity using the particle-resolved 3D regional model WRF-PartMC-MOSAIC.

References

Dockery, D. and A. Pope, 1996: Epidemiology of acute health effects: Summary of time-scale studies. *Particles in Our Air: Concentrations and Health Effects*, R. W. und J. Sprengler, Ed., Havard University Press, Cambridge, MA, 123–148.

Riemer, N. and M. West, 2013: Quantifying aerosol mixing state with entropy and diversity measures. *Atmospheric Chemistry and Physics*, **13 (22)**, 11 423–11 439.

Riemer, N., M. West, R. A. Zaveri, and R. C. Easter, 2009: Simulating the evolution of soot mixing state with a particle-resolved aerosol model. *J. Geophys. Res.*, **114**, D09 202, doi:10.1029/2008JD011073.

Stocker, T. F., et al., (Eds.), 2013: *Summary for Policymakers*, chap. SPM, 1–30. Cambridge University Press, doi:10.1017/CBO9781107415324.004.